



Ozone response to volcanic eruption

S. Muthers et al.

This discussion paper is/has been under review for the journal Atmospheric Chemistry and Physics (ACP). Please refer to the corresponding final paper in ACP if available.

The impact of volcanic aerosols on stratospheric ozone and the Northern Hemisphere polar vortex: separating radiative from chemical effects under different climate conditions

S. Muthers^{1,2}, F. Arfeuille³, C. C. Raible^{1,2}, and E. Rozanov^{4,5}

¹Climate and Environmental Physics, University of Bern, Bern, Switzerland

²Oeschger Centre for Climate Change Research, University of Bern, Bern, Switzerland

³Suisse Federal Laboratories for Material Science and Technology (Empa) Duebendorf, Switzerland

⁴Institute for Atmospheric and Climate Science, ETH, Zurich, Switzerland

⁵Physikalisch-Meteorologisches Observatorium Davos and World Radiation Center (PMOD/WRC), Davos, Switzerland

Title Page

Abstract

Introduction

Conclusions

References

Tables

Figures



Back

Close

Full Screen / Esc

Printer-friendly Version

Interactive Discussion



Received: 30 March 2015 – Accepted: 4 May 2015 – Published: 20 May 2015

Correspondence to: S. Muthers (muthers@climate.unibe.ch)

Published by Copernicus Publications on behalf of the European Geosciences Union.

ACPD

15, 14275–14314, 2015

Ozone response to volcanic eruption

S. Muthers et al.

Title Page

Abstract

Introduction

Conclusions

References

Tables

Figures



Back

Close

Full Screen / Esc

Printer-friendly Version

Interactive Discussion



Abstract

After strong volcanic eruptions stratospheric ozone changes are modulated by heterogeneous chemical reactions (HET) and dynamical perturbations related to the radiative heating in the lower stratosphere (RAD). Here, we assess the relative importance of both processes as well as the effect of the resulting ozone changes on the dynamics using ensemble simulations with the atmosphere–ocean–chemistry–climate model (AOCCM) SOCOL-MPIOM forced by eruptions with different strength. The simulations are performed under present day and preindustrial conditions to investigate changes in the response behaviour. The results show that the HET effect is only relevant under present day conditions and causes a pronounced global reduction of column ozone. These ozone changes further lead to a slight weakening of the Northern Hemisphere (NH) polar vortex during mid-winter. Independent from the climate state the RAD mechanism changes the column ozone pattern with negative anomalies in the tropics and positive anomalies in the mid-latitudes. The influence of the climate state on the RAD mechanism significantly differs in the polar latitudes, where an amplified ozone depletion during the winter months is simulated under present day conditions. This is in contrast to the preindustrial state showing a positive column ozone response also in the polar area. The dynamical response of the stratosphere is clearly dominated by the RAD mechanism showing an intensification of the NH polar vortex in winter. Still under present day conditions ozone changes due to the RAD mechanism slightly reduce the response of the polar vortex after the eruption.

1 Introduction

Tropical volcanic eruptions, which are strong enough to inject gases into the stratosphere, can perturb the physical and the chemical states of the climate system for several years and longer (Robock, 2000; Cole-Dai, 2010; Timmreck, 2012). Among the large number of eruption products, the sulphur dioxide (SO₂) has probably the

ACPD

15, 14275–14314, 2015

Ozone response to volcanic eruption

S. Muthers et al.

Title Page

Abstract

Introduction

Conclusions

References

Tables

Figures



Back

Close

Full Screen / Esc

Printer-friendly Version

Interactive Discussion



Ozone response to volcanic eruption

S. Muthers et al.

Title Page

Abstract

Introduction

Conclusions

References

Tables

Figures



Back

Close

Full Screen / Esc

Printer-friendly Version

Interactive Discussion



strongest climate impact. In the stratosphere SO_2 is converted into sulphuric acid ($\text{H}_2\text{SO}_4 + \text{H}_2\text{O}$) aerosols that (i) reflect in the visible part of the solar spectrum, (ii) absorb terrestrial and solar infrared radiation, and (iii) provide surface for a large number of chemical reactions that alter the chemical composition of the stratosphere (Forster et al., 2007). The aerosols increase the optical depth of the atmosphere, leading to a decrease in SW radiation in the troposphere and at the surface. The absorption of long wave radiation by the aerosols increases heating rates in the aerosol cloud, which leads to pronounced warming in these regions. The perturbed vertical and meridional temperature gradients affect the stratospheric circulation and by interaction between the stratosphere and the troposphere even the climate at the surface. A prominent example for this mechanism is the winter warming pattern in the NH that has been observed after several large tropical volcanic eruptions (Robock and Mao, 1992; Stenchikov et al., 2002; Shindell et al., 2004; Fischer et al., 2007; Christiansen, 2008; Zanchettin et al., 2012). Anomalous positive surface temperatures over Eurasia are related to a positive phase of the Arctic Oscillation, which is forced by the coupling of the stratospheric polar vortex and the tropospheric circulation (Graf et al., 1993; Kodera, 1994).

The effect of a tropical eruption on the stratospheric ozone chemistry can be further separated into (i) the effect of the changing temperature on the reaction rates, (ii) the heterogeneous chemistry on the sulphuric acid aerosols, (iii) the effect of the temperature changes and the aerosols on the polar stratospheric clouds (PSC), (iv) the changes induced by the dynamical perturbations in the stratosphere, and (v) changes in the photolysis rates. The temperature change and the reactions on the heterogeneous aerosol surfaces mainly take place in the aerosol cloud. In particular, the heterogeneous conversion of nitrogen oxides (N_2O_5) into nitric acid (HNO_3) is of importance. This reaction effectively slows down the NO_x cycle of catalytic ozone destruction with the effect of increasing ozone concentrations in the middle stratosphere, where the NO_x cycle dominates the depletion (Tie and Brasseur, 1995; Solomon et al., 1996). In the lower stratosphere, where the Cl_x and HO_x cycles are more important, the net-effect

Ozone response to volcanic eruption

S. Muthers et al.

Title Page

Abstract

Introduction

Conclusions

References

Tables

Figures



Back

Close

Full Screen / Esc

Printer-friendly Version

Interactive Discussion



is a reduction of the ozone abundance, since the slow-down of the NO_x cycle and heterogeneous reactions intensify the Cl_x and HO_x cycles (Tie and Brasseur, 1995; Solomon et al., 1996). In polar areas, the eruption is expected to intensify the ozone depletion. Firstly, with a stronger polar vortex the air temperature inside the vortex is reduced, better isolated from the mid latitudes, and more PSCs can be formed. Secondly, the presence of H_2SO_4 in the polar stratosphere facilitates the formation of an additional type of PSC, which further increases the surfaces for heterogeneous reactions on PSCs.

The net effect of the chemical response further depends on the background composition of the atmosphere. The slow-down of the NO_x cycle and heterogeneous reactions are expected to intensify the chlorine cycle of ozone destruction, but chlorine levels have undergone serious changes in the last decades (Solomon, 1999). With important quantities of additional anthropogenic ozone depleting halogens in the atmosphere the net effect of the eruption on the global ozone abundance is a reduction (Tie and Brasseur, 1995; Rozanov et al., 2002; Austin et al., 2013). For low halogen loadings, however, the chemical reactions are expected to increase ozone globally (Tie and Brasseur, 1995; Anet et al., 2013; Austin et al., 2013). Furthermore, increase in the stratospheric water vapour concentrations associated with the warming of the tropical tropopause can accelerate the HO_x cycle and reduce ozone even in the case of low halogen concentrations (Heckendorn et al., 2009).

The effect of a tropical eruption on stratospheric ozone can therefore be roughly divided into two processes. The first process involves changes in the radiation transfer through the atmosphere with the main effect of increased heating rates in the tropical lower stratosphere. This leads to pronounced changes in the dynamics, which change the meridional and vertical distribution of ozone. Furthermore, in regions with high optical depth the reduced incoming UV radiation can induce ozone depletion. The second process includes a large number of heterogeneous chemical reactions on the aerosol surface, which change the chemical composition of the stratosphere and strengthen or weaken different catalytic cycles of ozone destruction. In the following the first pro-

cess refers to the radiative effect of aerosols on the ozone chemistry (RAD), while the second process is named the chemical effect of aerosols (HET).

From the observations it is difficult to understand, which processes are responsible for the ozone changes and how these changes affect the dynamics. Using model simulations, the attribution of the ozone changes after the Mt. Pinatubo eruption has been assessed in several studies (Brasseur and Granier, 1992; Pitari and Rizi, 1993; Al-Saadi et al., 2001; Telford et al., 2009; Aquila et al., 2013). In general, they conclude that both mechanisms are important, with regional and seasonal differences.

In the tropics, total column ozone was reduced after the eruption of Mt. Pinatubo which was a combined signal of a reduction in the lower stratosphere and an increase of ozone concentrations above. The reduction in the lower stratosphere has been attributed to a mix of the dynamic effect and heterogeneous chemical reactions (Rosenfield et al., 1997; Rozanov et al., 2002). The former reduces ozone by enhanced upwelling of ozone poor air and the latter is responsible for an increase in the ozone depletion by active chlorine. Above 18 hPa the NO_x deactivation dominated, leading to positive ozone anomalies. Furthermore, Pitari and Rizi (1993) identified similar anomalies in the tropics related to changes in the UV radiation. A negative feedback between the tropical ozone changes and aerosol heating has been suggested by Al-Saadi et al. (2001), with an reduced heating of up to 25 % in the tropical middle stratosphere.

The differences in the ozone response between the NH and Southern Hemisphere (SH), i.e. a reduction in the NH but increasing ozone concentrations in the SH, has been attributed to dynamical processes induced by the aerosol heating in combination with the phase of the Brewer–Dobson circulation (Aquila et al., 2013) or the Quasi-Biennial Oscillation (QBO) (Telford et al., 2009; Randel and Wu, 1995). The ozone changes in the NH are primarily caused by the heterogeneous chemical reaction effects (Pitari and Rizi, 1993; Aquila et al., 2013), in particular at high latitudes (Portmann et al., 1996; Solomon et al., 1996; Rosenfield et al., 1997; Telford et al., 2009; Pitari et al., 2014).

The stratospheric dynamic perturbation after volcanic eruptions originates mainly from the aerosol heating in the tropical lower stratosphere. Nevertheless, changes in

Ozone response to volcanic eruption

S. Muthers et al.

Title Page

Abstract

Introduction

Conclusions

References

Tables

Figures



Back

Close

Full Screen / Esc

Printer-friendly Version

Interactive Discussion



Ozone response to volcanic eruption

S. Muthers et al.

Title Page

Abstract

Introduction

Conclusions

References

Tables

Figures



Back

Close

Full Screen / Esc

Printer-friendly Version

Interactive Discussion



the ozone concentrations also affect heating rates and therefore modulate the dynamic response to the eruption (Muthers et al., 2014a). Using observed ozone anomalies for the Mt. Pinatubo eruption, Stenchikov et al. (2002) found a strengthening of the Arctic Oscillation (AO) in late winter and early spring after the eruption, which is explained by the cooling effect of the polar stratospheric ozone depletion. However, by forcing the model with observed ozone anomalies, a separation of the dynamical and chemical causes of the ozone changes is not possible. Similar results were found by Shindell et al. (2003) who compared the Mt. Pinatubo eruption in simulations with and without ozone changes. For a different climate state (Mt. Tambora, 1815) without anthropogenic chlorine in the stratosphere, they found a very small influence of the ozone changes on the dynamical perturbation.

The purpose of this study is to deepen our understanding of the processes which drive ozone changes after a strong tropical volcanic eruption and how these changes modulate atmospheric dynamics in the stratosphere and troposphere. Moreover, we assess the influence of the eruption strength on these changes and the role of different climate states in moderating the dynamical responses. To the best of our knowledge these questions have not been addressed before. Here, we use a set of ensemble sensitivity simulations performed by the AOCCM SOCOL-MPIOM. To evaluate the dynamic response this study focuses mainly on the NH and on the winter season.

The paper is structured as follows: Sect. 2 introduces the coupled atmosphere–chemistry–ocean circulation model, the forcing data, and the setup of the experiments. The results are presented in Sect. 3, first for the simulated ozone changes associated with the different processes (Sect. 3.1), followed by the dynamical changes (Sect. 3.2). Section 3.3 focuses on interactions between the ozone chemistry and the dynamic response associated with the RAD effects. Finally, we discuss the results and present conclusive remarks in Sect. 4.

2 Model and experiments

2.1 SOCOL-MPIOM

SOCOL-MPIOM is a coupled atmosphere–ocean–chemistry–climate model (Muthers et al., 2014b). The atmospheric-chemistry component SOCOL version 3 (Schraner et al., 2008; Stenke et al., 2013) is based on the physical component MA-ECHAM5 (Roeckner et al., 2003; Manzini et al., 2006), which is coupled to the chemistry module MEZON (Rozanov et al., 1999; Egorova et al., 2003). The chemistry module uses temperature fields from ECHAM5 and calculates the tendency of 41 gas species, taking into account 200 gas-phase, 16 heterogeneous, and 35 photolytical reactions. Heterogeneous reactions are parametrised following Carslaw et al. (1995) and can take place in/on aqueous sulphuric acid aerosols and on three types of polar stratospheric clouds.

In the short-wave scheme of SOCOL the solar spectrum is divided into six spectral intervals. The scheme considers Rayleigh scattering, scattering on aerosols and clouds, and the absorption of solar irradiance in UV-induced photolysis reactions, by O₃, O₂, and 44 other species. In the near-infrared intervals absorption by water vapour, CO₂, N₂O, CH₄, and O₃ is implemented. Furthermore, a parametrisation for the absorption of radiation by O₂ and O₃ in the Lyman-alpha, Schumann-Runge, Hartley and Higgins bands is implemented following an approach similar to Egorova et al. (2004). The long-wave scheme considers frequencies from 10–3000 cm⁻¹ for the absorption by water vapour, CO₂, O₃, N₂O, CH₄, CFC-11, CFC-12, CFC-22, aerosols, and clouds. Chemistry–climate interactions can optionally be disabled in the model, by deactivating the interactive chemistry module. In this case three dimensional time dependent ozone data needs to be applied as forcing.

The spectral truncation used in this study is T31, which corresponds to a horizontal resolution of approximately 3.75° × 3.75°. In the vertical, the atmosphere is divided into 39 levels with the highest level at 0.01 hPa (80 km). With this vertical resolution the model is not able to produce a Quasi-Biennial Oscillation (QBO) by itself, therefore a QBO nudging is applied (Giorgetta et al., 1999).

Title Page

Abstract

Introduction

Conclusions

References

Tables

Figures



Back

Close

Full Screen / Esc

Printer-friendly Version

Interactive Discussion



Ozone response to volcanic eruption

S. Muthers et al.

Title Page

Abstract

Introduction

Conclusions

References

Tables

Figures



Back

Close

Full Screen / Esc

Printer-friendly Version

Interactive Discussion



The atmosphere-chemistry model SOCOL is coupled to the ocean model MPIOM which includes a sea ice module (Marsland, 2003; Jungclaus et al., 2006). MPIOM is used in a nominal resolution of 3° , with the poles shifted to Greenland and Antarctica to avoid numerical singularities at the poles. This setup allows for a high resolution in the deep water formation region of the North Atlantic. Both models, MPIOM and SOCOL are coupled by the OASIS3 coupler (Budich et al., 2010; Valcke, 2013).

2.2 Aerosol forcing data sets

In this study we assess the influence of radiative and chemical effects of stratospheric aerosols on stratospheric ozone chemistry and dynamics for different eruption sizes. To simulate the climatic effect of a volcanic eruption in SOCOL-MPIOM, the model needs information about the optical properties of the aerosols, including extinction coefficients, single scattering albedo, and the asymmetry factor for each spectral interval, latitude, vertical level, and time step. Furthermore, the chemistry module needs the surface area density (SAD) of the aerosols. In a sensitivity study for different eruption sizes, these forcings need to be generated in a consistent manner, to allow for a fair comparison between the eruptions.

Since nucleation, condensation, coagulation, and sedimentation of the aerosols change in different ways with the SO_2 concentration (Timmreck et al., 2010), a simple linear scaling of observation based aerosol data sets by the sulphur mass may lead to an unrealistic forcing data set. The aerosol coagulation process, for instance, depends on the SO_2 concentration and hence particles tend to be larger as we inject more SO_2 . The increase in total SAD is hence not proportional to the increase in SO_2 mass. Conversely, the total stratospheric warming depends on the aerosol absorption in the infrared and varies more or less linearly with the SO_2 mass injected. However, increase in the sedimentation rates with larger aerosols further modifies the relationship between the stratospheric warming and the initial sulphur mass released.

The aerosol data set used here, was therefore calculated offline using the micro-physical aerosol model AER (Weisenstein et al., 1997, 2007). AER is a 2-D model

Ozone response to volcanic eruption

S. Muthers et al.

Title Page

Abstract

Introduction

Conclusions

References

Tables

Figures



Back

Close

Full Screen / Esc

Printer-friendly Version

Interactive Discussion



with global domain, resolving the atmosphere from the surface to approximately 60 km altitude. The vertical resolution is about 1.2 km with a horizontal grid spacing of 9.5° of latitude. To simulate the formation of the aerosols the SO₂ injection mass, as well as the timing and latitude/altitude of the injection are used as inputs for the AER model.

5 Three AER simulations were carried out with 15, 30, and 60 Tg of SO₂ injected, the former corresponding approximately to the SO₂ detected in the stratosphere shortly after the Pinatubo eruption (Guo et al., 2004). Furthermore, the timing (mid of June) and the location (5° S–14° N between 23–25 km) are chosen to fit the Pinatubo 1991 eruption. Besides the sulphur mass, the same set of initial and boundary conditions
10 were applied in all three simulations, corresponding to the atmospheric state at the time of the eruption of Mt. Pinatubo in 1991 (Fleming et al., 1999).

SAD values and extinction coefficients in the visible are shown in Fig. 1 for the DJF season in the first winter after the eruption on the left and as Hovmoeller diagram for SAD and extinctions at 50 hPa on the right.

15 Note that Arfeuille et al. (2013) found that an injection of 14 Tg of SO₂ (7 Tg of sulphur) produced mid-visible extinctions much higher than observed in the tropical stratosphere after the Pinatubo eruption. As shown by Dhomse et al. (2014), the peak burden of sulphur in the particle phase was much lower than in the gas phase, in the range 3.7 to 6.7 Tg of sulphur. The 15 Tg AER simulation should therefore be regarded as
20 giving a stronger perturbation than occurred following Pinatubo. Using satellite based aerosol forcings, the agreement with observations could be improved for Pinatubo (Arfeuille et al., 2013). However, due to the non-linear relationship between sulphur mass and the aerosol properties the latter could not be used in this sensitivity study. A detailed comparison of satellite based aerosol data sets and the AER method is given in
25 Arfeuille et al. (2013).

2.3 Experiments

A number of ensemble sensitivity experiments were performed. The experiments differ in the aerosol forcing, the climate state, and the physical and chemical processes considered.

To assess the role of the climate state on the response, the eruptions either take place under present day conditions (early 1990s with high loads of ozone depleting substances (ODS) and greenhouse gases (GHG) in the atmosphere) or preindustrial conditions (early 19th century, low concentrations of ozone depleting halogens and GHG). Initial conditions for the two climate states are based on two transient simulations described in Muthers et al. (2014b). For the preindustrial climate state the restart files were selected between the years 1812 to 1814. Present day initial conditions were extracted between 1988 to 1990. Each ensemble consists of 8 simulations and the restart files were carefully selected to cover a wide range of different states of the Atlantic Meridional Overturning Circulation and the tropical Pacific (ENSO). The timing of the eruption (mid of June) is identical for both climate states.

For comparison, the simulated response of the climate system after the volcanic eruption is evaluated against an ensemble of control simulations for each climate state. These simulations were initialised using the same set of initial conditions, but were forced by an aerosol data set representing the unperturbed background state of the atmosphere.

To distinguish between the aerosol forcings and the climate states the simulations are named PI15, PI30, and PI60 for the eruption sizes of 15, 30, and 60 Tg of SO₂ in the preindustrial climate state, respectively. The present day simulations are named PD15, PD30, and PD60, accordingly. These simulations consider the both the radiative and the chemical aspects of the volcanic forcing (named full aerosol effect in the following). Therefore the model was forced with SAD values and optical properties generated by the AER model. Note, that the PD15 ensemble simulation closely resembles the conditions of the Mt. Pinatubo eruption in 1991. Moreover, the PI60 ensemble is

Ozone response to volcanic eruption

S. Muthers et al.

Title Page

Abstract

Introduction

Conclusions

References

Tables

Figures



Back

Close

Full Screen / Esc

Printer-friendly Version

Interactive Discussion



Ozone response to volcanic eruption

S. Muthers et al.

Title Page

Abstract

Introduction

Conclusions

References

Tables

Figures



Back

Close

Full Screen / Esc

Printer-friendly Version

Interactive Discussion



comparable to the Tambora eruption in 1815 (Gao et al., 2008) although the date of the eruption and the shape of the aerosol forcings is different (Arfeuille et al., 2014). All aerosol forcing time series were applied as zonal monthly means between 690 and 3.8 hPa and interpolated to the model levels in SOCOL-MPIOM.

Furthermore, the effect of stratospheric aerosols on the atmosphere will be separated into radiative perturbations (RAD) and changes related to heterogeneous chemical reactions (HET). In the RAD experiment, only the optical properties of the aerosols was applied as forcing and the pre-eruption values were used for the SAD. The HET experiment was forced only with time-varying SAD with the optical properties representing pre-eruptive conditions. Ensemble experiments for both processes were performed for the three eruption sizes of 15, 30, and 60 Tg of SO₂. In the following these experiments are identified by the suffix _HET and _RAD. A summary of the experiments used in this study is given in Table 1.

Finally, we extract the simulated ozone changes for the full forcing and RAD experiments and apply them as forcing in an additional set of ensemble simulations. A configuration of SOCOL-MPIOM without interactive chemistry is used in these experiments (Muthers et al., 2014b). Since ozone concentrations are not allowed to change, these simulations show the pure effect of the ozone changes on the dynamical perturbation. Consequently, aerosol forcings represent pre-eruptive conditions. Ozone concentrations are applied as daily mean values on the model grid, to avoid errors due to the vertical interpolation between pressure levels and model level. These experiments were performed for the 15 and 60 Tg aerosol forcing only.

The analysis presented mainly focuses on the first winter (DJF) after the eruption. Results are always expressed in terms of anomalies to the average of the control ensemble simulations for each climate state. Significance estimates are based on a two-tailed Student's t test.

3 Results

3.1 Ozone changes

The response of the global averaged column ozone (Fig. 2) reveals clear differences between the radiative and the chemical effects. In a present day climate state (Fig. 2 top) heterogeneous chemical reactions on the aerosol surface cause a depletion of global column ozone, which is significant for more than two years. Ozone is continuously reduced for about 9 month after the eruption, independent from the eruption size. However, the amplitude of the anomaly increases with the eruption size to -13 , -18 , and -21 DU. The recovery phase lasts about 24 months in all simulations, again independent of the eruption size. The spatial analysis of the anomalies reveals amplified ozone depletion in the high latitudes of both hemispheres, in particular during the winter months (Fig. 3a).

Zonally averaged height profiles for the first winter after the eruption reveal that the chemical effect also leads to positive anomalies in the upper stratosphere above 30 hPa (Fig. 4a). However, these anomalies are present only in the first winter after the eruption and are to some extent compensated by negative anomalies in the lower stratosphere. The positive anomalies in the upper stratosphere are related to the slow-down of the NO_x cycle of catalytic ozone destruction, as N_2O_5 is converted into HNO_3 on the H_2SO_4 aerosols. By reducing the NO_x concentrations the reaction also slows down the deactivation of chlorine, which dominates ozone destruction in the lower atmosphere and explains the negative anomalies below 30 hPa. Furthermore, the conversion stops, when all N_2O_5 is consumed. In the lower stratosphere N_2O_5 is quickly consumed in the months after the eruption, first in the tropical latitudes, but about 5 months after the eruptions N_2O_5 is reduced by more than 80 % at all latitudes below < 30 hPa. In the NH and SH polar stratosphere in late winter and spring the heterogeneous reactions on the aerosol surfaces and on PSCs strongly increase the chlorine concentrations in the lower stratosphere and explain the pronounced reductions of ozone.

Ozone response to volcanic eruption

S. Muthers et al.

Title Page

Abstract

Introduction

Conclusions

References

Tables

Figures

◀

▶

◀

▶

Back

Close

Full Screen / Esc

Printer-friendly Version

Interactive Discussion



Ozone response to volcanic eruption

S. Muthers et al.

Title Page

Abstract

Introduction

Conclusions

References

Tables

Figures



Back

Close

Full Screen / Esc

Printer-friendly Version

Interactive Discussion



The RAD effect causes positive global mean column ozone anomalies after the eruption, which peak about 7 months after the beginning of the eruption (+5, +8, and +12 DU), and return to background conditions after about 18 months (Fig. 2). Similar to the chemical effects, no clear differences in terms of the duration are found between the three eruption sizes. The column ozone anomaly time series furthermore reveal some fluctuations, mainly during the first year. In February–March and July–August, the positive column ozone anomalies undergo clear reductions. These variations are related to the present day polar ozone depletion in the NH and SH, which is further intensified after the eruption by colder conditions inside the polar vortices and chlorine activation on the PSCs. However, the polar ozone depletion in the RAD experiment is much weaker than the signal found in the HET ensemble experiment. For the 15 Tg aerosol forcing the polar ozone depletion is rather moderate (Fig. 3b), but the polar ozone depletion intensifies and lasts longer with increasing forcing strength.

Overall, the spatial pattern of ozone anomalies due to the RAD effect is more heterogeneous than for the HET effect (Fig. 3b). Reduced ozone column abundances are found at tropical latitudes and increasing concentrations at mid- to high-latitudes. The tropical reduction is related to pronounced ozone depletion at 30 hPa, which is partly compensated by positive ozone anomalies above and below (Fig. 4b). This equatorial anomaly pattern is very similar for all post-eruption seasons and remains significant until the end of the first year after the eruption. The circulation changes in the stratosphere that are responsible for the ozone anomalies are detected in the residual mean circulation anomaly (Andrews et al., 1987). The enhanced vertical transport of ozone changes the vertical ozone profile and replaces ozone enhanced air at 30 hPa by ozone depleted air from lower levels. Air with enriched ozone from 30 hPa further increases ozone concentrations at 10 hPa and above. The upward motion in the tropics is balanced by descending air masses in the mid-latitudes. Since these air masses originate from tropical latitudes, they transport ozone enriched air into the lower stratosphere of the mid-latitudes and create positive ozone anomalies. This meridional transport is visible in the positive anomalies of column ozone, which first occur in subtropical

Ozone response to volcanic eruption

S. Muthers et al.

Title Page

Abstract

Introduction

Conclusions

References

Tables

Figures



Back

Close

Full Screen / Esc

Printer-friendly Version

Interactive Discussion



latitudes and reach the high latitudes several months later. A fraction of descending ozone is recirculated into the lowermost tropical stratosphere and leads to positive ozone anomalies at 70 hPa. Furthermore, changes in the incoming UV radiation and photodissociation by the high optical depth of the aerosols may affect ozone production in the tropics (Pitari and Rizi, 1993), but this process is not yet implemented in the model.

The full aerosol effect displays the combined influence of both processes (Fig. 2). In the first 7 months after the eruption, radiative effects dominate the response of ozone with positive ozone anomalies, which reach maximum values of +2, +3, and +6 DU between autumn and early winter depending on the 15, 30, and 60 Tg forcing, respectively (Fig. 2). In the following, the influence of the radiative effects weakens, while chemical effects are still present and column ozone anomalies become negative for about two years. The imprint of the intensified polar ozone depletion is clearly visible in the full forcing experiment. With increasing eruption size the amplitude of the negative and positive anomalies increases, while the spatial patterns remain similar (Fig. 3e and d).

Changing the climatic background conditions from present day to preindustrial has a strong impact on the HET effect (Fig. 2 bottom and Fig. 3e). Without pronounced amounts of ODS in the stratosphere, the effect of heterogeneous chemical reactions on the chlorine cycle of ozone depletion is very weak. Instead, the slow-down of the NO_x cycle of ozone depletion becomes important, explaining slight positive anomalies of column ozone, for a few months after the eruption. However, with maximum anomalies between +4 to +5 DU the response is not very pronounced.

RAD effects introduce again positive anomalies of column ozone after the eruption (Figs. 2 and 3f). In comparison to the present day ensemble simulations, the anomalies are stronger, longer lasting and the variability is lower, which is explained by the reduced polar ozone depletion in a preindustrial atmosphere. In fact, the positive anomalies of column ozone cover all latitudes from the subtropics to polar areas (Fig. 3f). Consequently, the combined response is dominated by the radiative effect and the spatial

patterns of the anomaly are very similar (Fig. 3g). For larger eruption sizes, the amplitude of the ozone changes due to radiative effects increases, while heterogeneous chemical reactions are only marginally affected by the eruption strength (Fig. 2).

3.2 Temperature and dynamics

5 One motivation of this study is the question how ozone changes described in Sect. 3.1 modulate the dynamical perturbation of the stratosphere due to the volcanic eruption.

Temperature changes associated with an ozone loss due to the HET effect are small compared to the direct radiative effect, but significant temperature reductions are found in the present day climate state for all three eruption sizes. For the 15 Tg forcing the cooling reach a minimum of -1 K in the subtropical latitudes of both hemisphere in winter (Fig. 5a). These anomalies increase to more than -2 K for the 60 Tg forcing. The reduction of the meridional temperature gradient leads to a significant slow-down of the westerly circulation in the polar stratosphere during boreal winter (Fig. 6a) and a weakening of the polar vortex. As index for the NH polar vortex intensity, time series of the zonal mean wind component at 60° N and 10 hPa (Christiansen, 2001, 2005) are shown in Fig. 7. The weakening of this \bar{u}_{60} index due to the HET effect is mainly a phenomena of the mid-winter (December, January), while during late winter a slight, but not significant vortex intensification is found for the stronger forced ensemble simulations. This late winter intensification is probably related to the intensified ozone depletion and associated cooling at polar latitudes.

20 The RAD effects dominate for the temperature perturbations after the eruption. Significant positive temperature anomalies are found at almost all altitudes and latitudes, with the exception of the polar areas (Fig. 5b). As expected, the temperature anomalies increase with rising aerosol mass. From 15 to 30 Tg of SO_2 the temperature increase is almost linear, but for the 60 Tg eruption the temperature response seems to saturate. In the troposphere, the expected cooling due to the reduced incoming short-wave flux is found at tropical and subtropical latitudes. The stratospheric warming, however, causes only a weak intensification of the NH polar vortex (Figs. 6b and 7). Significant positive

Ozone response to volcanic eruption

S. Muthers et al.

Title Page

Abstract

Introduction

Conclusions

References

Tables

Figures



Back

Close

Full Screen / Esc

Printer-friendly Version

Interactive Discussion



Ozone response to volcanic eruption

S. Muthers et al.

[Title Page](#)[Abstract](#)[Introduction](#)[Conclusions](#)[References](#)[Tables](#)[Figures](#)[Back](#)[Close](#)[Full Screen / Esc](#)[Printer-friendly Version](#)[Interactive Discussion](#)

anomalies are found only for a short period in late winter in case of the 15 Tg aerosol forcing. In contrast the ensemble simulations with the 30 and 60 Tg aerosol forcings show a significant intensification of the vortex during most of the winter (Fig. 7).

The amplitude of the temperature change through the HET mechanism is much weaker than the changes caused by the RAD effect. Nevertheless, the temperature reduction causes a significant weakening of the NH polar vortex, but no significant increase is found in the RAD experiment for the 15 Tg aerosol forcing. The different dynamic responses are related to the different patterns of the temperature anomaly. The aerosol induced warming covers all latitudes up to 60° N in the lower and middle stratosphere and reaches even polar latitudes in the upper stratosphere. Contrary, the cooling associated with the HET effect is limited to latitudes < 30° N.

The combined influence of HET and RAD mechanisms is again visible in the full forcing experiment. The stratospheric warming is slightly reduced by heterogeneous chemical reactions and the dynamical changes are weaker in comparison to the RAD experiment (Fig. 6c). In particular the NH polar vortex weakening in mid-winter due to the HET effect is clearly visible in the $\bar{u}60$ index (Fig. 7).

Under preindustrial conditions the response to an eruption differs in several aspects. Similar to the ozone anomalies, the effect of heterogeneous chemical reactions on the stratospheric temperatures and dynamics is very small (Figs. 5e, 6e, and 7). No significant anomalies are found, not even for the strongest forcing scenario. RAD effects in a preindustrial atmosphere slightly differ from the response under present day conditions. The tropical stratospheric warming is weaker in the preindustrial atmosphere and differences in the temperature anomalies increase with eruption size. The stronger warming under preindustrial conditions is not related to the ozone changes in the RAD ensemble experiment, as will be shown below. A possible explanation could be found in the different background states. Due to the ozone depletion in the present day atmosphere, stratospheric ozone concentrations are substantially reduced in the present day tropical lower stratosphere. Furthermore, the increased GHGs concentrations differ between the two climate states and both effects lead to a colder tropical stratosphere

under present day conditions. With a colder stratosphere and a warmer troposphere the radiative heating from below is stronger in the present day climate state.

For the combined response in a preindustrial climate state no differences to the RAD results are found, neither for the 15 nor for the 60 Tg aerosol forcing.

5 A summary of the dynamical perturbation caused by RAD and HET and the role of the climate state and the eruption size is given in Fig. 8, which shows weakening or intensification of the meridional pressure gradient at 40 hPa and the stratospheric polar low. The HET mechanism leads to a reduction of the meridional pressure gradients under present day conditions, with significant anomalies between 0 and 40° N. Differences between the eruption sizes are not found. Under preindustrial conditions, ozone changes due to heterogeneous chemical reactions have no significant influence on the meridional gradient.

10 The radiative effect of the aerosols increases the pressure gradient in both climate states. Geopotential height differences between low and high latitudes increase with eruption size, although not in a linear way. The anomalies are significant from the equator to the northern mid latitudes, but not in the polar area. The weakening of the stratospheric polar low is therefore not significant, not even for the strongest eruptions size. The full aerosol effect on the meridional geopotential height gradient is in all cases very similar to the radiative effects.

20 **3.3 Contributions from chemistry–climate interactions**

The simulated ozone changes due to the RAD effect or in the combined response could amplify or weaken the dynamical perturbation of the stratosphere. However, from the results described above, possible feedbacks between the ozone chemistry and the dynamics are difficult to extract. Two additional sensitivity ensemble experiments were therefore performed, driven only by the simulated ensemble mean ozone changes obtained from the RAD and full forcing experiments, which were shown for instance in Figs. 2 and 3.

Ozone response to volcanic eruption

S. Muthers et al.

Title Page

Abstract

Introduction

Conclusions

References

Tables

Figures



Back

Close

Full Screen / Esc

Printer-friendly Version

Interactive Discussion



Ozone response to volcanic eruption

S. Muthers et al.

Title Page

Abstract

Introduction

Conclusions

References

Tables

Figures



Back

Close

Full Screen / Esc

Printer-friendly Version

Interactive Discussion



Zonal mean temperature anomalies (Fig. 9) reveal an amplification of the aerosol-induced warming in the lower tropical stratosphere by the ozone chemistry. At these levels, ozone anomalies up to 0.2 ppmv (25 %) are found in the PD15_RAD ensemble mean, resulting in temperature anomalies of about 1.2 ± 0.3 K (80 hPa) during the first winter season after the eruption. Ozone anomalies and temperature anomalies increase with eruption size and reach 0.4 ppmv and 2.9 ± 0.5 K for the 60 Tg eruption in a present day climate state. For the ozone changes extracted from the full forcing experiment, the impact on tropical stratospheric temperatures is always weaker, due to the ozone depleting effect of heterogeneous chemical reactions. Under preindustrial conditions, the response is slightly stronger, but the differences are not significant.

RAD ozone changes in the tropics furthermore produce a cooling above 30 hPa with temperature anomalies from -2 K (15 Tg) to -4 K (60 Tg). Ozone changes in this region therefore weaken the warming effect of the aerosols. Heterogeneous chemical reactions have no effect on temperatures in this region and ozone changes from the RAD and the full forcing ensemble simulations lead to very similar temperature patterns. Temperature anomalies in a preindustrial atmosphere do not significantly differ from the results obtained under present day conditions. Note, that the cold anomaly in the upper stratosphere and mesosphere (present in all panels of Fig. 9) can not be attributed to volcanic induced ozone anomalies but is related to the missing diurnal cycle of ozone variations in SOCOL-MPIOM without interactive chemistry (Muthers et al., 2014b).

Furthermore, positive temperature anomalies are found in the NH polar stratosphere, though not significant except for one experiment (ozone changes from PD15_RAD). Since ozone anomalies in the NH polar stratosphere are very weak during the first winter after an eruption, these warm anomalies are probably not related to the ozone chemistry, but to dynamical changes.

The effect of the ozone perturbations on the NH polar vortex is in general small (Fig. 7) and not always consistent. Nevertheless, all experiments under present day conditions reveal a slight weakening of the vortex, which is significant for a few days in

mid-winter. The response of the vortex is weaker and not significant when ensemble simulations under preindustrial conditions are considered.

4 Discussion and conclusions

This study addresses the role of ozone changes for the dynamical perturbations of the stratosphere after strong tropical volcanic eruptions. Thereby, the underlying mechanisms and the influence of the climate state and the eruption strengths are considered. The results are based on a number of ensemble sensitivity simulations with the AOCCM SOCOL-MPIOM, which allows us to separate the effect of heterogeneous chemical reactions from the warming effect of the aerosols for two different climate states and three different eruption intensities.

In agreement with earlier studies we find that both processes, heterogeneous chemical reactions on the aerosol surface and the warming effect of the aerosols are important for the ozone changes after the eruption in an atmosphere with enhanced concentrations of ODS (Pitari and Rizzi, 1993; Al-Saadi et al., 2001). The chemical effect, however, is the dominant one with a pronounced global reduction of the total column ozone after the eruption, when the atmosphere contains high loads of ODS. Regionally, the warming effect can become more important, for instance in the tropics and mid latitudes, where dynamical changes cause pronounced negative (equator) and positive (subtropics) anomalies of column ozone. Under preindustrial conditions with low load of ozone depleting halogens, the chemical effects become very weak and the response is dominated by the aerosol warming.

The dynamical perturbation of the stratosphere is dominated by the radiative effects of the aerosols. During winter time, the warming in the tropical stratosphere increases the meridional temperature gradient towards the poles and strengthens the westerly circulation in the polar stratosphere. Ozone changes, related to heterogeneous chemical reactions under present day climatic conditions have been shown to weaken the warming in the tropical stratosphere and the NH polar vortex. Contrary, ozone changes

Ozone response to volcanic eruption

S. Muthers et al.

Title Page

Abstract

Introduction

Conclusions

References

Tables

Figures



Back

Close

Full Screen / Esc

Printer-friendly Version

Interactive Discussion



related to the RAD mechanism amplify the warming in the lower stratosphere, but weaken the temperature response in the middle stratosphere. The latter causes a slight weakening of the polar vortex.

The climate state influences the response of the ozone chemistry and the dynamical response to the volcanic aerosols in a significant way. As already shown by Tie and Brasseur (1995) heterogeneous chemical reactions on the aerosol surface cause pronounced global ozone depletion when stratospheric loads of ozone depleting halogens are high, but has only a weak positive effect in a preindustrial atmosphere. Furthermore, ozone depletion scales with the amplitude of eruptions in a present day climate state, but for preindustrial conditions the response is independent from the eruption size (Tie and Brasseur, 1995). With the projected reduction of ODS (Austin and Wilson, 2006; Eyring et al., 2007; Austin et al., 2010) the effect of heterogeneous chemical reactions can be expected to become less important for future eruptions. However, differences in the background state affect the results of this study as well. In recent decades, the stratosphere has undergone a pronounced cooling trend (e.g., Thompson et al., 2012), related to the ozone changes and the increasing levels of GHG (Shine et al., 2003). This cooling also affects the meridional temperature profiles in the stratosphere and the dynamics. In this study, significant differences in the vortex behaviour exist between the control simulations for preindustrial and present day and these differences are often larger, than the differences between the simulations perturbed by the volcanic eruption.

A direct comparison of our results to observations is difficult given the highly idealised character of our experiments. Nevertheless, one experiment, the 15 Tg experiment for the full aerosol effects in a present day climate state, is characterised by very similar boundary conditions as the eruption of Pinatubo in 1991. Globally, the combined aerosol effect for the 15 Tg aerosol forcing results in an ozone loss of 10.4 ± 3.7 DU 21 months after the start of the eruption. This agrees reasonably well with observations for Pinatubo (Bodeker et al., 2005), where a reduction of -13.9 DU was observed peaking in May 1993 (22 months after the eruption). Furthermore, the pattern of column

Ozone response to volcanic eruption

S. Muthers et al.

Title Page

Abstract

Introduction

Conclusions

References

Tables

Figures



Back

Close

Full Screen / Esc

Printer-friendly Version

Interactive Discussion



Ozone response to volcanic eruption

S. Muthers et al.

Title Page

Abstract

Introduction

Conclusions

References

Tables

Figures



Back

Close

Full Screen / Esc

Printer-friendly Version

Interactive Discussion



ozone anomalies in Bodeker et al. (2005) is similar to the pattern found in the PD15 ensemble mean (Fig. 3). After the eruption, negative anomalies are found in the tropics and positive anomalies in the mid latitudes. The magnitude of both is stronger in SOCOL-MPIOM than in observations. In particular, the positive column ozone anomaly in the NH mid-latitudes is weaker in the Bodeker et al. (2005) data set. This may be related to the QBO effect (Telford et al., 2009; Randel and Wu, 1995) or the Brewer–Dobson circulation (Aquila et al., 2013), which modulated the ozone anomalies after Pinatubo. The modulating effect of the QBO, however, has been removed by the comparison to an ensemble of control simulations nudged by the same QBO reconstruction. Overestimated ozone anomalies in the PD15 ensemble may further be related to the too strong warming simulated in the tropical stratosphere by SOCOL-MPIOM. The remaining anomalies, i.e., the polar ozone depletion and the global reduction of columns ozone about one year after the eruptions agrees reasonable well with the simulated anomalies. For the vertical pattern of ozone changes (e.g., Hassler et al., 2008) the agreement between model results and observations is also reasonable, with the exception of stronger anomalies in the model, in particular in the tropics.

A caveat of this study is the overestimated warming in the tropical stratosphere, which may leads to an overestimation of the dynamical response and the resulting ozone changes. This needs to be considered, when interpreting the results of the RAD and full forcing ensemble results. An overestimation of the lower stratospheric warming after volcanic eruptions is a feature common to many models (e.g. Driscoll et al., 2012). The maximum warming after the Pinatubo eruption in a multi-model ensemble average of 13 CMIP5 models (model selection as in Driscoll et al., 2012) is 3.8 ± 2.9 K for the temperature anomaly at 50 hPa, while reanalysis products and observations suggest temperature anomalies between 2.5 and 3 K (Labitzke and McCormick, 1992; Dee et al., 2011). However, the phase of the QBO and other dynamical processes are suggested to reduce the stratospheric warming after Pinatubo (Driscoll et al., 2012; Fueglistaler et al., 2014). SOCOL-MPIOM simulates a warming of 8.7 ± 1.2 K in the PD15 ensemble. Our results show that the overestimated warming is to some extent

Ozone response to volcanic eruption

S. Muthers et al.

Title Page

Abstract

Introduction

Conclusions

References

Tables

Figures



Back

Close

Full Screen / Esc

Printer-friendly Version

Interactive Discussion



related to the ozone changes, which amplify the warming by about 1.5 K (15 Tg forcing). Furthermore, the aerosol forcing applied in this study contributes to the overestimated warming. We use an aerosol forcing produced by an aerosol micro-physical model, which allows us to generate physical consistent forcing for different eruption intensities. This model-generated forcing differs from satellite based observations for Pinatubo in several aspects (as described by Arfeuille et al., 2013). For comparison, we also perform eight simulations forced by realistic satellite based aerosol concentrations for the Mt. Pinatubo eruption (SAGE_4λ in Arfeuille et al., 2013). In these simulations (not shown) the stratospheric warming is still overestimated (maximum temperature anomalies: 6.0 ± 1.0 K), but the agreement to other CMIP5 is better, in particular when the temperature effect of the ozone changes is considered.

In summary, we show that ozone changes after strong tropical volcanic eruptions play a minor role for the dynamical perturbation of the stratosphere although for in some cases (e.g., high load of ODS) a weak influence is detectable. Nevertheless, this influence is small compared to the radiative effect of the aerosols.

Acknowledgements. This work has been supported by the Swiss National Science Foundation under grant CRSII2-147659 (FUPSOL II) and profited from discussions during the PAGES/FUPSOL Workshop in 2014.

References

- Al-Saadi, J. A., Pierce, R. B., Fairlie, T. D., Kleb, K. M., Eckman, R. S., Grose, W. L., Natarajan, M., and Olson, J. R.: Response of middle atmosphere chemistry and dynamics to volcanically elevated sulfate aerosol: three-dimensional coupled model simulations, *J. Geophys. Res.*, 106, 27255–27275, doi:10.1029/2000JD000185, 2001. 14280, 14294
- Andrews, D. G., Holton, J. R., and Leovy, C. B.: *Middle Atmosphere Dynamics*, Academic Press, Orlando, USA, 1987. 14288, 14309
- Anet, J. G., Muthers, S., Rozanov, E., Raible, C. C., Peter, T., Stenke, A., Shapiro, A. I., Beer, J., Steinhilber, F., Brönnimann, S., Arfeuille, F., Brugnara, Y., and Schmutz, W.: Forcing

Ozone response to volcanic eruption

S. Muthers et al.

Title Page

Abstract

Introduction

Conclusions

References

Tables

Figures



Back

Close

Full Screen / Esc

Printer-friendly Version

Interactive Discussion



of stratospheric chemistry and dynamics during the Dalton Minimum, *Atmos. Chem. Phys.*, 13, 10951–10967, doi:10.5194/acp-13-10951-2013, 2013. 14279

Aquila, V., Oman, L. D., Stolarski, R., Douglass, A. R., and Newman, P. A.: The response of ozone and nitrogen dioxide to the eruption of Mt. Pinatubo at southern and northern midlatitudes, *J. Atmos. Sci.*, 70, 894–900, doi:10.1175/JAS-D-12-0143.1, 2013. 14280, 14296

Arfeuille, F., Luo, B. P., Heckendorn, P., Weisenstein, D., Sheng, J. X., Rozanov, E., Schraner, M., Brönnimann, S., Thomason, L. W., and Peter, T.: Modeling the stratospheric warming following the Mt. Pinatubo eruption: uncertainties in aerosol extinctions, *Atmos. Chem. Phys.*, 13, 11221–11234, doi:10.5194/acp-13-11221-2013, 2013. 14284, 14297

Arfeuille, F., Weisenstein, D., Mack, H., Rozanov, E., Peter, T., and Brönnimann, S.: Volcanic forcing for climate modeling: a new microphysics-based data set covering years 1600–present, *Clim. Past*, 10, 359–375, doi:10.5194/cp-10-359-2014, 2014. 14286

Austin, J. and Wilson, R. J.: Ensemble simulations of the decline and recovery of stratospheric ozone, *J. Geophys. Res.*, 111, D16314, doi:10.1029/2005JD006907, 2006. 14295

Austin, J., Scinocca, J., Plummer, D., Oman, L., Waugh, D., Akiyoshi, H., Bekki, S., Braesicke, P., Butchart, N., Chipperfield, M., Cugnet, D., Dameris, M., Dhomse, S., Eyring, V., Frith, S., Garcia, R. R., Garny, H., Gettelman, A., Hardiman, S. C., Kinnison, D., Lamarque, J. F., Mancini, E., Marchand, M., Michou, M., Morgenstern, O., Nakamura, T., Pawson, S., Pitari, G., Pyle, J., Rozanov, E., Shepherd, T. G., Shibata, K., Teyssède, H., Wilson, R. J., and Yamashita, Y.: Decline and recovery of total column ozone using a multimodel time series analysis, *J. Geophys. Res.*, 115, D00M10, doi:10.1029/2010JD013857, 2010. 14295

Austin, J., Horowitz, L. W., Schwarzkopf, M. D., Wilson, R. J., and Levy, H.: Stratospheric ozone and temperature simulated from the preindustrial era to the present day, *J. Climate*, 26, 3528–3543, doi:10.1175/JCLI-D-12-00162.1, 2013. 14279

Bodeker, G. E., Shiona, H., and Eskes, H.: Indicators of Antarctic ozone depletion, *Atmos. Chem. Phys.*, 5, 2603–2615, doi:10.5194/acp-5-2603-2005, 2005. 14295, 14296

Brasseur, G. and Granier, C.: Mount Pinatubo aerosols, chlorofluorocarbons, and ozone depletion, *Science*, 257, 1239–42, doi:10.1126/science.257.5074.1239, 1992. 14280

Budich, R., Gioretta, M., Jungclaus, J., Redler, R., and Reick, C.: The MPI-M Millennium Earth System Model: an assembling guide for the COSMOS configuration, MPI report, Max-Planck Institute for Meteorology, Hamburg, Germany, 2010. 14283

Ozone response to volcanic eruption

S. Muthers et al.

Title Page

Abstract

Introduction

Conclusions

References

Tables

Figures



Back

Close

Full Screen / Esc

Printer-friendly Version

Interactive Discussion



- Carlsaw, K. S., Luo, B., and Peter, T.: An analytic expression for the composition of aqueous aerosols including gas phase removal of HNO_3 - H_2SO_4 stratospheric aerosols including gas phase removal of HNO_3 , *Geophys. Res. Lett.*, 22, 1877–1880, 1995. 14282
- Christiansen, B.: Downward propagation of zonal mean zonal wind anomalies from the stratosphere to the troposphere: model and reanalysis, *J. Geophys. Res.*, 106, 27307, doi:10.1029/2000JD000214, 2001. 14290
- Christiansen, B.: Downward propagation and statistical forecast of the near-surface weather, *J. Geophys. Res.*, 110, D14104, doi:10.1029/2004JD005431, 2005. 14290
- Christiansen, B.: Volcanic eruptions, large-scale modes in the Northern Hemisphere, and the El Niño-Southern Oscillation, *J. Climate*, 21, 910–922, doi:10.1175/2007JCLI1657.1, 2008. 14278
- Cole-Dai, J.: Volcanoes and climate, *Wiley Interdisciplinary Reviews: Climate Change*, 1, 824–839, doi:10.1002/wcc.76, 2010. 14277
- Dee, D. P., Uppala, S. M., Simmons, A. J., Berrisford, P., Poli, P., Kobayashi, S., Andrae, U., Balmaseda, M. A., Balsamo, G., Bauer, P., Bechtold, P., Beljaars, A. C. M., van de Berg, L., Bidlot, J., Bormann, N., Delsol, C., Dragani, R., Fuentes, M., Geer, A. J., Haimberger, L., Healy, S. B., Hersbach, H., Hólm, E. V., Isaksen, I., Kållberg, P., Köhler, M., Matricardi, M., McNally, A. P., Monge-Sanz, B. M., Morcrette, J.-J., Park, B.-K., Peubey, C., de Rosnay, P., Tavolato, C., Thépaut, J.-N., and Vitart, F.: The ERA-Interim reanalysis: configuration and performance of the data assimilation system, *Q. J. Roy. Meteor. Soc.*, 137, 553–597, doi:10.1002/qj.828, 2011. 14296
- Dhomse, S. S., Emmerson, K. M., Mann, G. W., Bellouin, N., Carlsaw, K. S., Chipperfield, M. P., Hommel, R., Abraham, N. L., Telford, P., Braesicke, P., Dalvi, M., Johnson, C. E., O'Connor, F., Morgenstern, O., Pyle, J. A., Deshler, T., Zawodny, J. M., and Thomason, L. W.: Aerosol microphysics simulations of the Mt. Pinatubo eruption with the UM-UKCA composition-climate model, *Atmos. Chem. Phys.*, 14, 11221–11246, doi:10.5194/acp-14-11221-2014, 2014. 14284
- Driscoll, S., Bozzo, A., Gray, L. J., Robock, A., and Stenchikov, G.: Coupled Model Intercomparison Project 5 (CMIP5) simulations of climate following volcanic eruptions, *J. Geophys. Res.*, 117, D17105, doi:10.1029/2012JD017607, 2012. 14296
- Egorova, T., Rozanov, E., Zubov, V., and Karol, I. L.: Model for Investigating Ozone Trends (MEZON), *Izv. Atmos. Ocean. Phys.*, 39, 277–292, 2003. 14282

Ozone response to volcanic eruption

S. Muthers et al.

Title Page

Abstract

Introduction

Conclusions

References

Tables

Figures



Back

Close

Full Screen / Esc

Printer-friendly Version

Interactive Discussion



Egorova, T., Rozanov, E., Manzini, E., Schmutz, W., and Peter, T.: Chemical and dynamical response to the 11-year variability of the solar irradiance simulated with a chemistry–climate model, *Geophys. Res. Lett.*, 83, 6225–6230, 2004. 14282

5 Eyring, V., Waugh, D. W., Bodeker, G. E., Cordero, E., Akiyoshi, H., Austin, J., Beagley, S. R., Boville, B. A., Braesicke, P., Brühl, C., Butchart, N., Chipperfield, M. P., Dameris, M., Deckert, R., Deushi, M., Frith, S. M., Garcia, R. R., Gettelman, A., Giorgetta, M. A., Kinnison, D. E., Mancini, E., Manzini, E., Marsh, D. R., Matthes, S., Nagashima, T., Newman, P. A., Nielsen, J. E., Pawson, S., Pitari, G., Plummer, D. A., Rozanov, E., Schraner, M., Scinocca, J. F., Semeniuk, K., Shepherd, T. G., Shibata, K., Steil, B., Stolarski, R. S., Tian, W., and Yoshiki, M.: Multimodel projections of stratospheric ozone in the 21st century, *J. Geophys. Res.*, 112, D16303, doi:10.1029/2006JD008332, 2007. 14295

10 Fischer, E. M., Luterbacher, J., Zorita, E., Tett, S. F. B., Casty, C., and Wanner, H.: European climate response to tropical volcanic eruptions over the last half millennium, *Geophys. Res. Lett.*, 34, 1–6, doi:10.1029/2006GL027992, 2007. 14278

15 Fleming, E. L., Jackman, H., Stolarski, S., and Considine, D. B.: Simulation of stratospheric tracers using an improved empirically based two-dimensional model transport formulation and equatorial, *J. Geophys. Res.*, 104, 23911–23934, doi:10.1029/1999JD900332, 1999. 14284

20 Forster, P., Ramaswamy, V., Artaxo, P., Bernsten, T., Betts, R., Fahey, D. W., Haywood, J., Lean, J., Lowe, D. C., Myhre, G., Nganga, J., Prinn, R., Raga, G., Schulz, M., and Van Dorland, R.: Changes in Atmospheric Constituents and in Radiative Forcing, chap. 2, Cambridge University Press, Cambridge, United Kingdom, New York, 2007. 14278

Fueglistaler, S., Abalos, M., Flannaghan, T. J., Lin, P., and Randel, W. J.: Variability and trends in dynamical forcing of tropical lower stratospheric temperatures, *Atmos. Chem. Phys.*, 14, 13439–13453, doi:10.5194/acp-14-13439-2014, 2014. 14296

25 Gao, C., Robock, A., and Ammann, C.: Volcanic forcing of climate over the past 1500 years: an improved ice core-based index for climate models, *J. Geophys. Res.*, 113, D23111, doi:10.1029/2008JD010239, 2008. 14286

Giorgetta, M. A., Bengtsson, L., and Arpe, K.: An investigation of QBO signals in the east Asian and Indian monsoon in GCM experiments, *Clim. Dynam.*, 15, 435–450, doi:10.1007/s003820050292, 1999. 14282

30 Graf, H.-F., Kirchner, I., Robock, A., and Schult, I.: Pinatubo eruption winter climate effects: model versus observations, *Clim. Dynam.*, 92, 81–93, 1993. 14278

Ozone response to volcanic eruption

S. Muthers et al.

Title Page

Abstract

Introduction

Conclusions

References

Tables

Figures



Back

Close

Full Screen / Esc

Printer-friendly Version

Interactive Discussion



Guo, S., Rose, W. I., Bluth, G. J. S., and Watson, I. M.: Particles in the great Pinatubo volcanic cloud of June 1991: the role of ice, *Geochem. Geophys. Geosy.*, 5, 1–35, doi:10.1029/2003GC000655, 2004. 14284

Hassler, B., Bodeker, G. E., and Dameris, M.: Technical Note: A new global database of trace gases and aerosols from multiple sources of high vertical resolution measurements, *Atmos. Chem. Phys.*, 8, 5403–5421, doi:10.5194/acp-8-5403-2008, 2008. 14296

Heckendorn, P., Weisenstein, D., Fueglistaler, S., Luo, B. P., Rozanov, E., Schraner, M., Thomason, L. W., and Peter, T.: The impact of geoengineering aerosols on stratospheric temperature and ozone, *Environ. Res. Lett.*, 4, 045108, doi:10.1088/1748-9326/4/4/045108, 2009. 14279

Jungclaus, J. H., Keenlyside, N., Botzet, M., Haak, H., Luo, J.-J., Latif, M., Marotzke, J., Mikolajewicz, U., and Roeckner, E.: Ocean circulation and tropical variability in the coupled model ECHAM5/MPI-OM, *J. Climate*, 19, 3952–3972, doi:10.1175/JCLI3827.1, 2006. 14283

Kodera, K.: Influence of volcanic eruptions on the troposphere through stratospheric dynamical processes in the Northern Hemisphere winter, *J. Geophys. Res.*, 99, 1273–1282, 1994. 14278

Labitzke, K. and McCormick, M. P.: Stratospheric temperature increases due to Pinatubo aerosols, *Geophys. Res. Lett.*, 19, 207–210, 1992. 14296

Manzini, E., Giorgetta, M. A., Esch, M., Kornblueh, L., and Roeckner, E.: The influence of sea surface temperatures on the northern winter stratosphere: ensemble simulations with the MAECHAM5 model, *J. Climate*, 19, 3863–3881, doi:10.1175/JCLI3826.1, 2006. 14282

Marsland, S.: The Max-Planck-Institute global ocean/sea ice model with orthogonal curvilinear coordinates, *Ocean Model.*, 5, 91–127, doi:10.1016/S1463-5003(02)00015-X, 2003. 14283

Muthers, S., Anet, J. G., Raible, C. C., Brönnimann, S., Rozanov, E., Arfeuille, F., Peter, T., Shapiro, A. I., Beer, J., Steinhilber, F., Brugnara, Y., and Schmutz, W.: Northern hemispheric winter warming pattern after tropical volcanic eruptions: sensitivity to the ozone climatology, *J. Geophys. Res.*, 110, 1340–1355, doi:10.1002/2013JD020138, 2014a. 14281

Muthers, S., Anet, J. G., Stenke, A., Raible, C. C., Rozanov, E., Brönnimann, S., Peter, T., Arfeuille, F. X., Shapiro, A. I., Beer, J., Steinhilber, F., Brugnara, Y., and Schmutz, W.: The coupled atmosphere–chemistry–ocean model SOCOL-MPIOM, *Geosci. Model Dev.*, 7, 2157–2179, doi:10.5194/gmd-7-2157-2014, 2014b. 14282, 14285, 14286, 14293

Ozone response to volcanic eruption

S. Muthers et al.

Title Page

Abstract

Introduction

Conclusions

References

Tables

Figures



Back

Close

Full Screen / Esc

Printer-friendly Version

Interactive Discussion



- Pitari, G. and Rizi, V.: An estimate of the chemical and radiative perturbation of stratospheric ozone following the eruption of Mt. Pinatubo, *J. Atmos. Sci.*, 50, 3260–3276, 1993. 14280, 14289, 14294
- Pitari, G., Aquila, V., Kravitz, B., Robock, A., Watanabe, S., Cionni, I., De Luca, N., Di Genova, G., Mancini, E., and Tilmes, S.: Stratospheric ozone response to sulfate geoengineering: results from the Geoengineering Model Intercomparison Project (GeoMIP), *J. Geophys. Res.*, 119, 2629–2653, doi:10.1002/2013JD020566, 2014. 14280
- Portmann, R. W., Solomon, S., Garcia, R. R., Thomason, L. W., Poole, L. R., and McCormick, M. P.: Role of aerosol variations in anthropogenic ozone depletion in the polar regions paper, *J. Geophys. Res.*, 101, 22991–23,006, doi:10.1029/96JD02608, 1996. 14280
- Randel, W. J. and Wu, F.: Ozone and temperature changes in the stratosphere following the eruption of Mount Pinatubo, *J. Geophys. Res.*, 100, 16753–16764, doi:10.1029/95JD01001, 1995. 14280, 14296
- Robock, A.: Volcanic eruptions and climate, *Rev. Geophys.*, 38, 191–219, 2000. 14277
- Robock, A. and Mao, J.: Winter warming from large volcanic eruptions, *Geophys. Res. Lett.*, 12, 2405–2408, 1992. 14278
- Roeckner, E., Bäuml, G., Bonaventura, L., Brokopf, R., Esch, M., Giorgetta, M., Hagemann, S., Kirchner, I., Kornbluh, L., Manzini, E., Rhodin, A., Schlese, U., Schulzweida, U., and Tompkins, A.: The atmospheric general circulation model ECHAM5 – model description, MPI report 349, Max-Planck Institute for Meteorology, Hamburg, Germany, 2003. 14282
- Rosenfield, J. E., Considine, D. C., Meade, P. E., Bacmeister, J. T., Jackman, C. H., and Schoeberl, M. R.: Stratospheric effects of Mount Pinatubo aerosol studied with a coupled two-dimensional model, *J. Geophys. Res.*, 102, 3649–3670, doi:10.1029/96JD03820, 1997. 14280
- Rozanov, E., Schlesinger, M. E., Zubov, V., Yang, F., and Andronova, N. G.: The UIUC three-dimensional stratospheric chemical transport model: description and evaluation of the simulated source gases and ozone, *J. Geophys. Res.*, 104, 11755–11781, doi:10.1029/1999JD900138, 1999. 14282
- Rozanov, E. V., Schlesinger, M. E., Andronova, N. G., Yang, F., Malyshev, S. L., Zubov, V. A., Egorova, T. A., and Li, B.: Climate/chemistry effects of the Pinatubo volcanic eruption simulated by the UIUC stratosphere/troposphere GCM with interactive photochemistry, *J. Geophys. Res.*, 107, ACL 12–1–ACL 12–14, doi:10.1029/2001JD000974, 2002. 14279, 14280

Ozone response to volcanic eruption

S. Muthers et al.

Title Page

Abstract

Introduction

Conclusions

References

Tables

Figures



Back

Close

Full Screen / Esc

Printer-friendly Version

Interactive Discussion



- Schraner, M., Rozanov, E., Schnadt Poberaj, C., Kenzelmann, P., Fischer, A. M., Zubov, V., Luo, B. P., Hoyle, C. R., Egorova, T., Fueglistaler, S., Brönnimann, S., Schmutz, W., and Peter, T.: Technical Note: Chemistry-climate model SOCOL: version 2.0 with improved transport and chemistry/microphysics schemes, *Atmos. Chem. Phys.*, 8, 5957–5974, doi:10.5194/acp-8-5957-2008, 2008. 14282
- 5 Shindell, D. T., Schmidt, G. A., Miller, R. L., and Mann, M. E.: Volcanic and solar forcing of climate change during the preindustrial era, *J. Climate*, 16, 4094–4107, doi:10.1175/1520-0442(2003)016<4094:VASFOC>2.0.CO;2, 2003. 14281
- Shindell, D. T., Schmidt, G. A., Mann, M. E., and Faluvegi, G.: Dynamic winter climate response to large tropical volcanic eruptions since 1600, *J. Geophys. Res.*, 109, D05104, doi:10.1029/2003JD004151, 2004. 14278
- 10 Shine, K. P., Bourqui, M. S., Forster, P. M. D. F., Hare, S. H. E., Langematz, U., Braesicke, P., Grewe, V., Ponater, M., Schnadt, C., Smith, C. A., Haigh, J. D., Austin, J., Butchart, N., Shindell, D. T., Randel, W. J., Nagashima, T., Portmann, R. W., Solomon, S., Seidel, D. J., Lanzante, J., Klein, S., Ramaswamy, V., and Schwarzkopf, M. D.: A comparison of model-simulated trends in stratospheric temperatures, *Q. J. Roy. Meteor. Soc.*, 129, 1565–1588, doi:10.1256/qj.02.186, 2003. 14295
- Solomon, S.: Stratospheric ozone depletion: a review of concepts and history, *Rev. Geophys.*, 37, 275, doi:10.1029/1999RG900008, 1999. 14279
- 20 Solomon, S., Portmann, R. W., Garcia, R. R., Thomason, L. W., Poole, L. R., McCormick, M. P., and Cly, C.: The role of aerosol variations in anthropogenic ozone depletion at northern midlatitudes, *J. Geophys. Res.*, 101, 6713–6727, 1996. 14278, 14279, 14280
- Stenchikov, G., Robock, A., Ramaswamy, V., Schwarzkopf, M. D., Hamilton, K., and Ramachandran, S.: Arctic Oscillation response to the 1991 Mount Pinatubo eruption: effects of volcanic aerosols and ozone depletion, *J. Geophys. Res.*, 107, 1–16, doi:10.1029/2002JD002090, 2002. 14278, 14281
- 25 Stenke, A., Schraner, M., Rozanov, E., Egorova, T., Luo, B., and Peter, T.: The SOCOL version 3.0 chemistry–climate model: description, evaluation, and implications from an advanced transport algorithm, *Geosci. Model Dev.*, 6, 1407–1427, doi:10.5194/gmd-6-1407-2013, 2013. 14282
- Telford, P., Braesicke, P., Morgenstern, O., and Pyle, J.: Reassessment of causes of ozone column variability following the eruption of Mount Pinatubo using a nudged CCM, *Atmos. Chem. Phys.*, 9, 4251–4260, doi:10.5194/acp-9-4251-2009, 2009. 14280, 14296

Ozone response to volcanic eruption

S. Muthers et al.

Title Page

Abstract

Introduction

Conclusions

References

Tables

Figures



Back

Close

Full Screen / Esc

Printer-friendly Version

Interactive Discussion



Thompson, D. W. J., Seidel, D. J., Randel, W. J., Zou, C.-Z., Butler, A. H., Mears, C., Osso, A., Long, C., and Lin, R.: The mystery of recent stratospheric temperature trends, *Nature*, 491, 692–697 2012. 14295

Tie, X. and Brasseur, G.: The response of stratospheric ozone to volcanic eruptions: sensitivity to atmospheric chlorine loading, *Geophys. Res. Lett.*, 22, 3035–3038, 1995. 14278, 14279, 14295

Timmreck, C.: Modeling the climatic effects of large explosive volcanic eruptions, *Wiley Interdisciplinary Reviews: Climate Change*, 3, 545–564, doi:10.1002/wcc.192, 2012. 14277

Timmreck, C., Graf, H.-F., Lorenz, S. J., Niemeier, U., Zanchettin, D., Matei, D., Jungclaus, J. H., and Crowley, T. J.: Aerosol size confines climate response to volcanic super-eruptions, *Geophys. Res. Lett.*, 37, 1–5, doi:10.1029/2010GL045464, 2010. 14283

Valcke, S.: The OASIS3 coupler: a European climate modelling community software, *Geosci. Model Dev.*, 6, 373–388, doi:10.5194/gmd-6-373-2013, 2013. 14283

Weisenstein, D. K., Yue, G. K., Ko, M. K. W., Sze, N. D., Rodriguez, J. M., and Scott, C. J.: A two-dimensional model of sulfur species and aerosols, *J. Geophys. Res.*, 102, 13019–13035, 1997. 14283

Weisenstein, D. K., Penner, J. E., Herzog, M., and Liu, X.: Global 2-D intercomparison of sectional and modal aerosol modules, *Atmos. Chem. Phys.*, 7, 2339–2355, doi:10.5194/acp-7-2339-2007, 2007. 14283

Zanchettin, D., Timmreck, C., Bothe, O., Lorenz, S. J., Hegerl, G., Graf, H.-F., Luterbacher, J., and Jungclaus, J. H.: Delayed winter warming: a robust decadal response to strong tropical volcanic eruptions?, *Geophys. Res. Lett.*, 40, 204–209, doi:10.1029/2012GL054403, 2012. 14278

Ozone response to volcanic eruption

S. Muthers et al.

Table 1. Overview of the ensemble experiments used in this study. SO₂ mass refers to the aerosol amount assumed in the generation of the volcanic forcing (compare Sect. 2.2). Climate state: PD: 1990s conditions with high concentrations of ozone depleting substances (ODS). PI: preindustrial atmosphere with low concentrations of ODS. Volcanic forcing: SAD: surface area density of the aerosols. OP: optical properties, i.e., extinction rates for all spectral intervals. For each ensemble, 8 simulations are performed.

Ensemble	SO ₂ mass [Tg]	Climate state	Volcanic forcing	Atm. chemistry
PD[15,30,60]	15, 30, 60	PD	SAD and OP	interactive
PI[15,30,60]	15, 30, 60	PI	SAD and OP	interactive
PD[15,30,60]_HET	15, 30, 60	PD	SAD	interactive
PI[15,30,60]_HET	15, 30, 60	PI	SAD	interactive
PD[15,30,60]_RAD	15, 30, 60	PD	OP	interactive
PI[15,30,60]_RAD	15, 30, 60	PI	OP	interactive
PD[15,60]_o3	15, 60	PD	–	ozone from PD[15,60]
PI[15,60]_o3	15, 60	PI	–	ozone from PI[15,60]
PD[15,60]RAD_o3	15, 60	PD	–	ozone from PD[15,60]_RAD
PI[15,60]RAD_o3	15, 60	PI	–	ozone from PI[15,60]_RAD
PD_CTRL	–	PD	–	interactive
PI_CTRL	–	PI	–	interactive

Title Page

Abstract

Introduction

Conclusions

References

Tables

Figures

◀

▶

◀

▶

Back

Close

Full Screen / Esc

Printer-friendly Version

Interactive Discussion



Ozone response to volcanic eruption

S. Muthers et al.

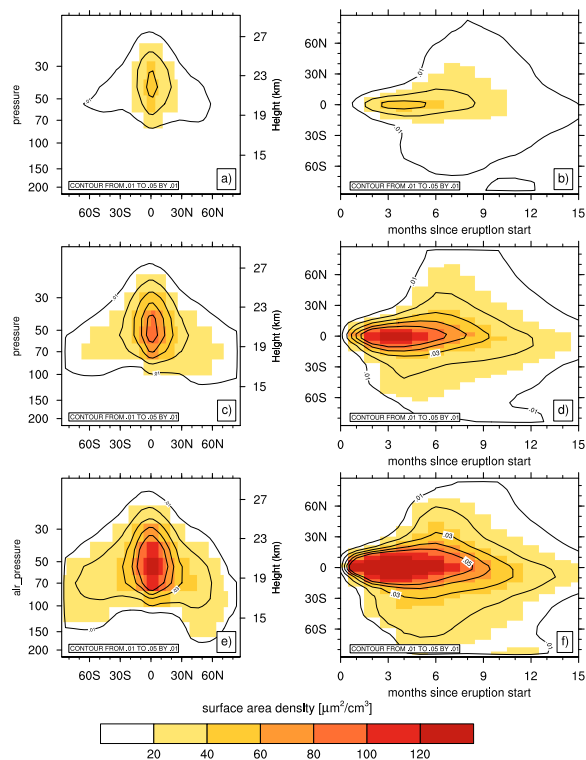


Figure 1. Aerosol data sets used in the simulations for the 15 Tg (**a, b**), 30 Tg (**c, d**), and 60 Tg (**e, f**) SO₂ aerosol forcing. Surface area densities (SAD) are displayed by colours; contours denote extinction rates in the visible (440–690 nm) with contours from 0 to 0.05 by an interval of 0.01 km⁻¹. The column on the left displays averages for the first post-eruption winter season (DJF) as a function of pressure and latitude, while the right column shows Hovmöller diagrams of the monthly mean SAD forcing at 50 hPa.

Title Page

Abstract

Introduction

Conclusions

References

Tables

Figures



Back

Close

Full Screen / Esc

Printer-friendly Version

Interactive Discussion



Ozone response to volcanic eruption

S. Muthers et al.

Title Page

Abstract

Introduction

Conclusions

References

Tables

Figures



Back

Close

Full Screen / Esc

Printer-friendly Version

Interactive Discussion

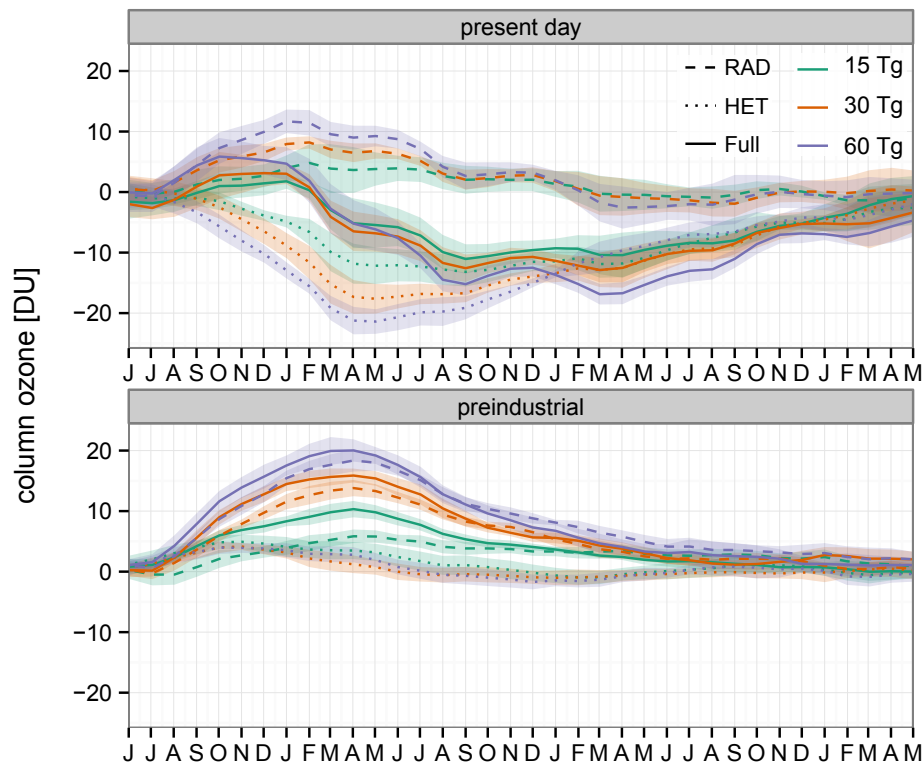


Figure 2. Monthly mean global mean anomalies of column ozone [DU] in a present day (top) and preindustrial climate state (bottom) for the ensemble simulations with the full forcing effect (Full, solid lines), the ensemble simulations considering only the chemical effect of the aerosols (HET, dotted lines), and the simulations forced only by the radiative aerosol effects (RAD, dashed lines). The different eruption sizes are indicated by colours. Lines denote the ensemble mean, shading the standard deviation (SD) of the ensemble.

Ozone response to volcanic eruption

S. Muthers et al.

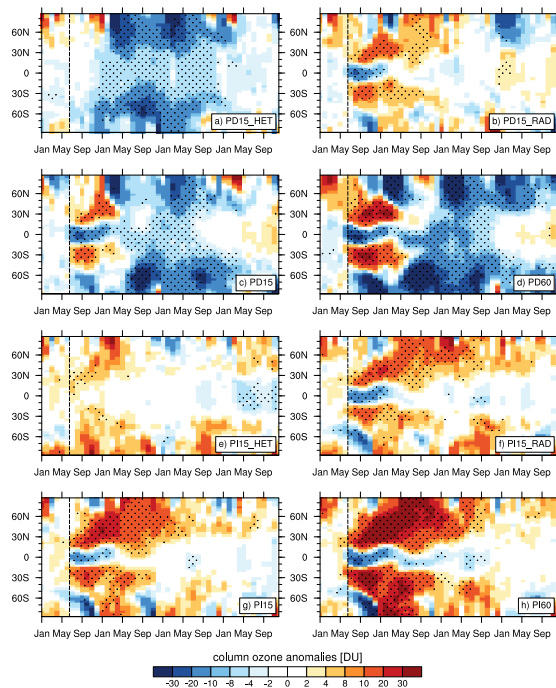


Figure 3. Zonal average monthly mean anomalies of total columns ozone [DU] between January of the eruption year (year 0) and 40 months after the eruption in different ensemble simulations: **(a)** anomalies due to the effect of heterogeneous chemical reactions for the 15 Tg eruption in a present day climate state. **(b)** Same as **(a)**, but for the radiative effects of the aerosols. **(c)** Same as **(a)**, but for the full forcing simulations. **(d)** Full forcing simulations for the 60 Tg aerosol forcing data set. **(e–h)** Similar to **(a–d)**, but for the preindustrial climate state. Anomalies are calculated relatively to the corresponding control ensemble mean and the stippling in the simulation panels indicates significant differences to the control (Student's t test $p \leq 0.05$). The beginning of the eruption is depicted by the vertical dashed line.

Ozone response to volcanic eruption

S. Muthers et al.

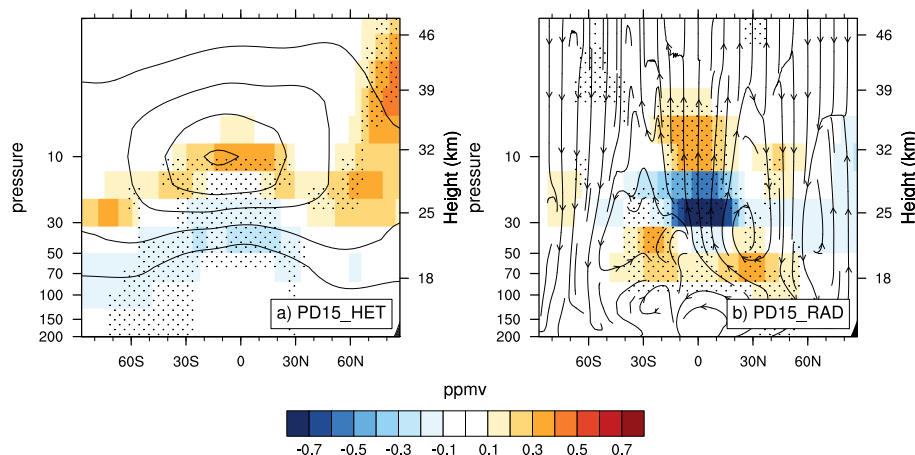


Figure 4. Ensemble mean zonal mean ozone mixing ratio anomalies [ppmv] for the first post eruption DJF season in the present day ensemble experiment considering (a) the effect of heterogeneous chemical reactions (b) the radiative effect with the 15 Tg aerosol forcing under present day conditions. Contour lines in (a) denote the climatological average DJF ozone mixing ratios in the present day control ensemble. The streamlines in (b) show the residual circulation anomalies (Andrews et al., 1987). Stippling indicates significant anomalies (Student's *t* test $p \leq 0.05$).

Title Page

Abstract

Introduction

Conclusions

References

Tables

Figures

◀

▶

◀

▶

Back

Close

Full Screen / Esc

Printer-friendly Version

Interactive Discussion



Ozone response to volcanic eruption

S. Muthers et al.

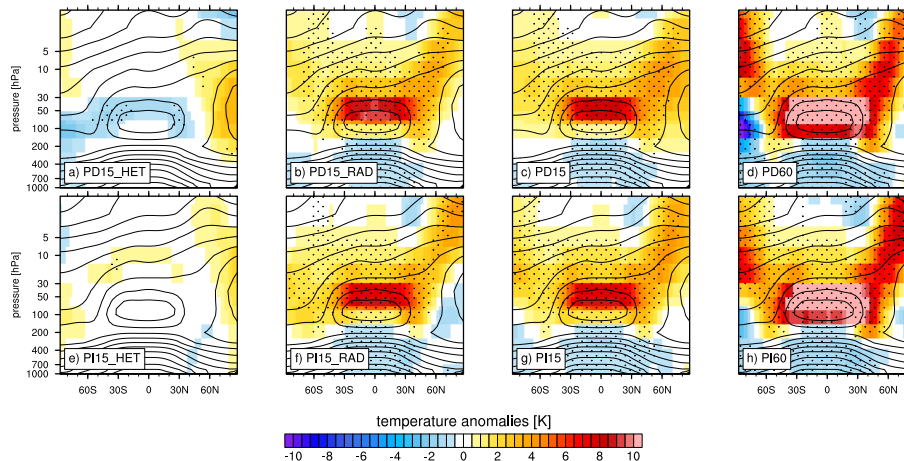


Figure 5. Zonal mean temperature anomalies [K] for the first post eruption winter (DJF) relative to the average of the present day or preindustrial control simulations: **(a)** anomalies due to the effect of heterogeneous chemical reactions (HET) for the 15 Tg eruption in a present day climate state, **(b)** same as **(a)**, but for the radiative effects of the aerosols, **(c)** same as **(a)**, but showing the ensemble mean of the full forcing simulations, **(d)** full forcing simulations for the 60 Tg aerosol forcing data set, and **(e–h)** similar to **(a)**, but for the preindustrial climate state. Anomalies are calculated relatively to the corresponding control ensemble mean and the stippling in the simulation panels indicates significant differences to the control (student's t test $p \leq 0.05$). Contours denote the climatological mean DJF temperatures in the control ensembles.

Title Page

Abstract

Introduction

Conclusions

References

Tables

Figures

◀

▶

◀

▶

Back

Close

Full Screen / Esc

Printer-friendly Version

Interactive Discussion



Ozone response to volcanic eruption

S. Muthers et al.

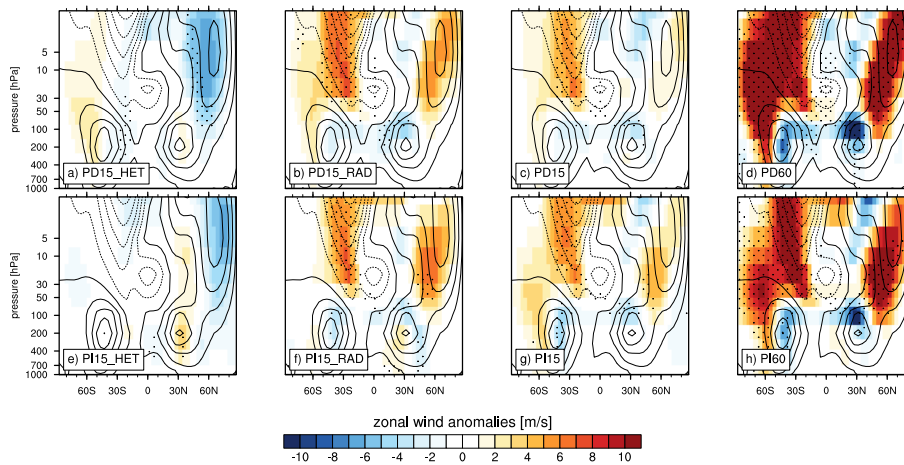


Figure 6. Similar to Fig. 5, but for the zonal mean zonal wind anomalies [m s^{-1}].

[Title Page](#)[Abstract](#)[Introduction](#)[Conclusions](#)[References](#)[Tables](#)[Figures](#)[Back](#)[Close](#)[Full Screen / Esc](#)[Printer-friendly Version](#)[Interactive Discussion](#)

Ozone response to volcanic eruption

S. Muthers et al.

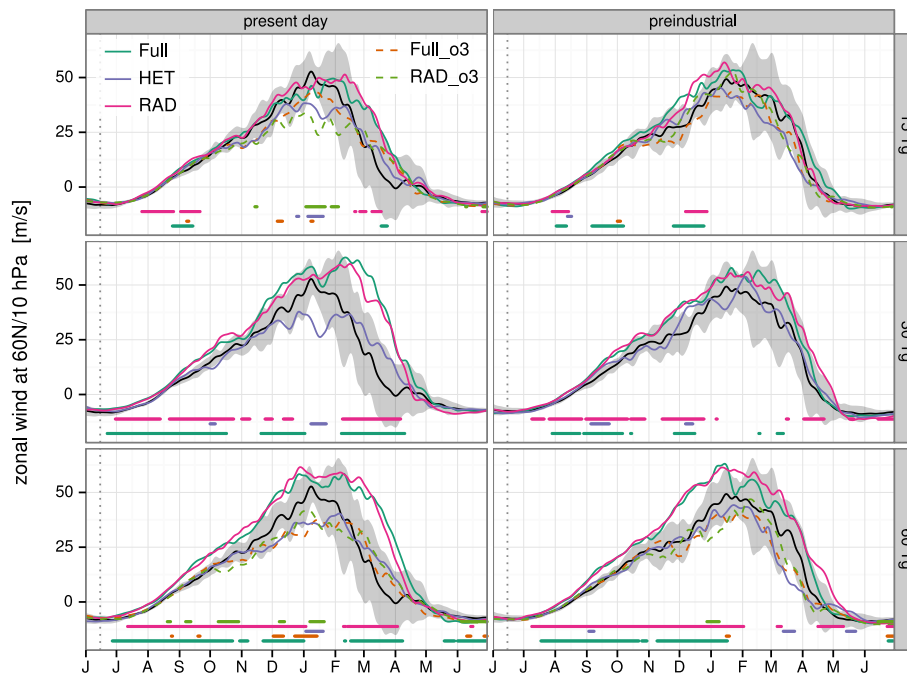


Figure 7. Daily zonal mean zonal wind at 60° N [m s^{-1}] used as index for the NH polar vortex intensity. Dots at the bottom of each panel indicate days with significant differences to the control ensemble ($p \leq 0.05$). All values are smoothed with an 11 day low pass filter. The start of the eruption (mid of June) is indicated by the vertical dashed line. The shading indicates the SD in the control experiments.

Title Page

Abstract

Introduction

Conclusions

References

Tables

Figures



Back

Close

Full Screen / Esc

Printer-friendly Version

Interactive Discussion



Ozone response to volcanic eruption

S. Muthers et al.

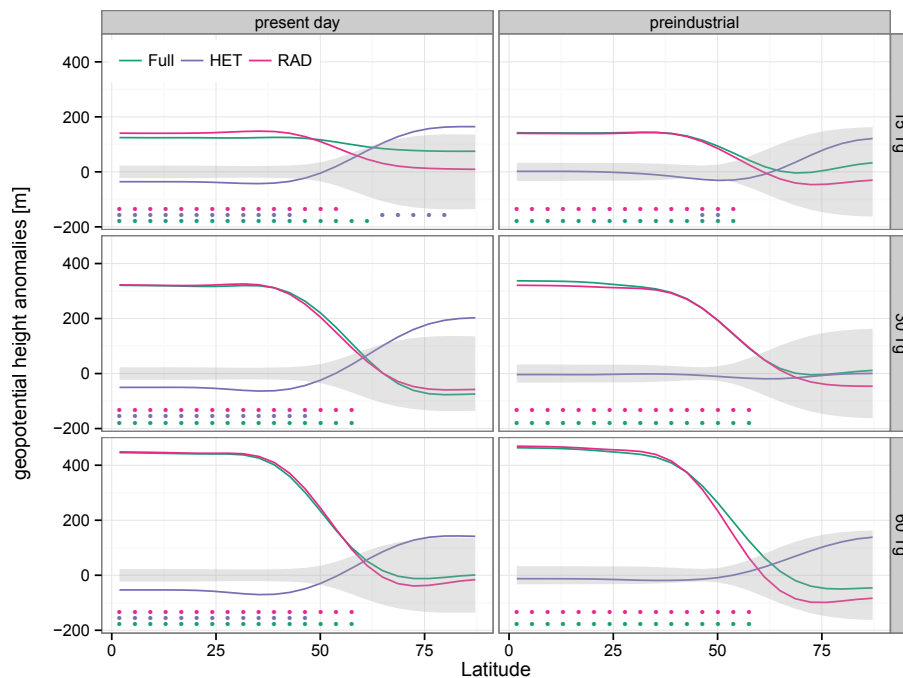


Figure 8. Zonal mean geopotential height anomalies [m] at 40 hPa for the first post eruption DJF season relative to the average of the present day or preindustrial control simulations. The grey shading indicates the SD in the control experiments. Dots at the bottom of each panel indicate significant differences to the corresponding control ensemble ($p \leq 0.05$).

Title Page

Abstract

Introduction

Conclusions

References

Tables

Figures

◀

▶

◀

▶

Back

Close

Full Screen / Esc

Printer-friendly Version

Interactive Discussion



Ozone response to volcanic eruption

S. Muthers et al.

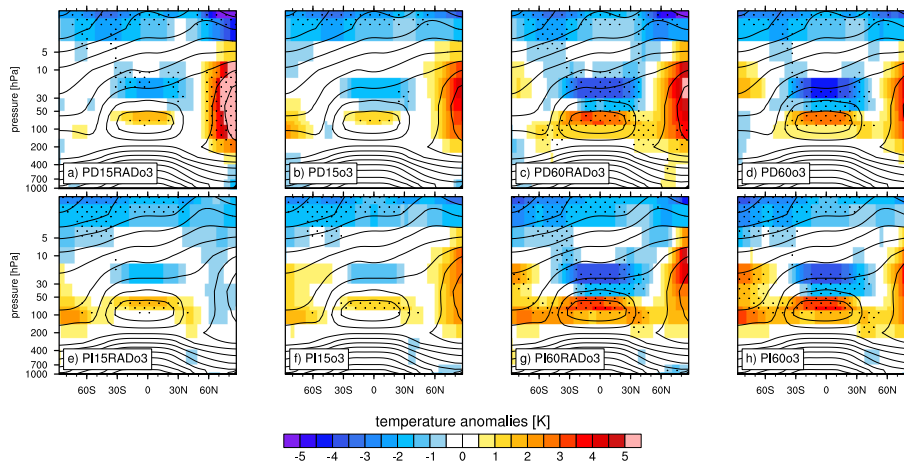


Figure 9. Similar to Fig. 5 but showing DJF zonal mean temperature anomalies [K] in the ozone sensitivity ensemble experiment. (top) present day ensemble experiments forced by ozone changes from PD15_RAD (a), PD15 (b), PD60_RAD (c), and PD60 (d). (bottom) Same forcings but for the preindustrial climate state experiments. Note the different colour scaling in comparison to Fig. 5.

[Title Page](#)[Abstract](#)[Introduction](#)[Conclusions](#)[References](#)[Tables](#)[Figures](#)[Back](#)[Close](#)[Full Screen / Esc](#)[Printer-friendly Version](#)[Interactive Discussion](#)